Synthesis of high-order bandpass filters based on coupled-resonator optical waveguides (CROWs)

Hsi-Chun Liu* and Amnon Yariv

Department of Electrical Engineering, California Institute of Technology, Pasadena, California 91125, USA
**hliu@caltech.edu*

Abstract: We present a filter design formalism for the synthesis of coupled-resonator optical waveguide (CROW) filters. This formalism leads to expressions and a methodology for deriving the coupling coefficients of CROWs for the desired filter responses and is based on coupled-mode theory as well as the recursive properties of the coupling matrix. The coupling coefficients are universal and can be applied to various types of resonators. We describe a method for the conversion of the coupling coefficients to the parameters based on ring resonators and grating defect resonators. The designs of Butterworth and Bessel CROW filters are demonstrated as examples.

OCIS codes: (130.2790) Guided waves; (130.3120) Integrated optical devices; (130.7408) Wavelength filtering devices; (230.4555) Coupled resonators.

References and links

1. A. Yariv, Y. Xu, R. K. Lee, and A. Scherer, "Coupled-resonator optical waveguide: a proposal and analysis," Opt. Lett. **24**(11), 711–713 (1999).
2. J. K. S. Poon, L. Zhu, G. A. DeRose, and A. Yariv, "Transmission and group delay of microring coupled-resonator optical waveguides," Opt. Lett. **31**(4), 456–458 (2006).
3. F. N. Xia, L. Sekaric, and Y. Vlasov, "Ultracompact optical buffers on a silicon chip," Nat. Photonics **1**(1), 65–71 (2007).
4. S. Nishikawa, S. Lan, N. Ikeda, Y. Sugimoto, H. Ishikawa, and K. Asakawa, "Optical characterization of photonic crystal delay lines based on one-dimensional coupled defects," Opt. Lett. **27**(23), 2079–2081 (2002).
5. M. Notomi, E. Kuramochi, and T. Tanabe, "Large-scale arrays of ultrahigh-Q coupled nanocavities," Nat. Photonics **2**(12), 741–747 (2008).
6. R. S. Tucker, P. C. Ku, and C. J. Chang-Hasnain, "Slow-light optical buffers: capabilities and fundamental limitations," J. Lightwave Technol. **23**(12), 4046–4066 (2005).
7. A. Melloni, F. Morichetti, and M. Martinelli, "Four-wave mixing and wavelength conversion in coupled-resonator optical waveguides," J. Opt. Soc. Am. B **25**(12), C87–C97 (2008).
8. P. Chak and J. E. Sipe, "Minimizing finite-size effects in artificial resonance tunneling structures," Opt. Lett. **31**(17), 2568–2570 (2006).
9. M. Sumetsky and B. J. Eggleton, "Modeling and optimization of complex photonic resonant cavity circuits," Opt. Express **11**(4), 381–391 (2003).
10. J. Capmany, P. Muñoz, J. D. Domenech, and M. A. Muriel, "Apodized coupled resonator waveguides," Opt. Express **15**(16), 10196–10206 (2007).
11. C. K. Madsen and J. H. Zhao, *Optical Filter Design and Analysis, A Signal Processing Approach* (Wiley, 1999).
12. B. E. Little, S. T. Chu, P. P. Absil, J. V. Hryniewicz, F. G. Johnson, E. Seiferth, D. Gill, V. Van, O. King, and M. Trakalo, "Very high-order microring resonator filters for WDM applications," IEEE Photon. Technol. Lett. **16**(10), 2263–2265 (2004).
13. F. N. Xia, M. Rooks, L. Sekaric, and Y. Vlasov, "Ultra-compact high order ring resonator filters using submicron silicon photonic wires for on-chip optical interconnects," Opt. Express **15**(19), 11934–11941 (2007).
14. P. Dong, N. N. Feng, D. Z. Feng, W. Qian, H. Liang, D. C. Lee, B. J. Luff, T. Banwell, A. Agarwal, P. Toliver, R. Menendez, T. K. Woodward, and M. Asghari, "GHz-bandwidth optical filters based on high-order silicon ring resonators," Opt. Express **18**(23), 23784–23789 (2010).
15. Q. Li, M. Soltani, S. Yegnanarayanan, and A. Adibi, "Design and demonstration of compact, wide bandwidth coupled-resonator filters on a siliconon- insulator platform," Opt. Express **17**(4), 2247–2254 (2009).
16. S. J. Xiao, M. H. Khan, H. Shen, and M. H. Qi, "A highly compact third-order silicon microring add-drop filter with a very large free spectral range, a flat passband and a low delay dispersion," Opt. Express **15**(22), 14765–14771 (2007).

#151208 - $15.00 USD Received 18 Jul 2011; revised 9 Aug 2011; accepted 10 Aug 2011; published 23 Aug 2011

17. H. A. Haus and Y. Lai, "Theory of cascaded quarter wave shifted distributed feedback resonators," IEEE J. Quantum Electron. **28**(1), 205–213 (1992).
18. D. Park, S. Kim, I. Park, and H. Lim, "Higher order optical resonant filters based on coupled defect resonators in photonic crystals," J. Lightwave Technol. **23**(5), 1923–1928 (2005).
19. R. Orta, P. Savi, R. Tascone, and D. Trinchero, "Synthesis of multiple-ring-resonator filters for optical systems," IEEE Photon. Technol. Lett. **7**(12), 1447–1449 (1995).
20. B. E. Little, S. T. Chu, H. A. Haus, J. Foresi, and J. P. Laine, "Microring resonator channel dropping filters," J. Lightwave Technol. **15**(6), 998–1005 (1997).
21. V. Van, "Circuit-based method for synthesizing serially coupled microring filters," J. Lightwave Technol. **24**(7), 2912–2919 (2006).
22. A. Melloni and M. Martinelli, "Synthesis of direct-coupled-resonators bandpass filters for WDM systems," J. Lightwave Technol. **20**(2), 296–303 (2002).
23. J. K. S. Poon and A. Yariv, "Active coupled-resonator optical waveguides. I. Gain enhancement and noise," J. Opt. Soc. Am. B **24**(9), 2378–2388 (2007).
24. H. A. Haus, *Waves and Fields in Optoelectronics* (Prentice-Hall, 1984).
25. A. M. Prabhu and V. Van, "Predistortion techniques for synthesizing coupled microring filters with loss," Opt. Commun. **281**(10), 2760–2767 (2008).
26. J. K. S. Poon, J. Scheuer, S. Mookherjea, G. T. Paloczi, Y. Y. Huang, and A. Yariv, "Matrix analysis of microring coupled-resonator optical waveguides," Opt. Express **12**(1), 90–103 (2004).
27. A. Martínez, J. García, P. Sanchis, F. Cuesta-Soto, J. Blasco, and J. Martí, "Intrinsic losses of coupled-cavity waveguides in planar-photonic crystals," Opt. Lett. **32**(6), 635–637 (2007).
28. A. Yariv and P. Yeh, *Photonics*, 6th ed. (Oxford University Press, 2007).

1. Introduction

A coupled-resonator optical waveguide (CROW) consists of a chain of weakly coupled resonators in which light propagates by virtue of the coupling between adjacent resonators [1]. Such a waveguiding mechanism is unique and can be realized in various types of resonators, such as ring resonators [2,3], grating resonators [4], and 2D photonic crystal resonators [5]. One of the key features of CROWs is that optical pulses can propagate at a significantly reduced group velocity, dictated by the inter-resonator coupling. This ability to "slow" down light may find applications such as optical delay lines, optical buffers, interferometers, and nonlinear optics [3,6,7].

The first proposal and analysis of CROWs was based on infinite-length chains whose dispersion properties can be derived and are controlled by essentially a single parameter, the coupling coefficient κ [1]. In practice, an infinite-length CROW has to be terminated and coupled to the outside world. The resulting finite-length CROW requires a proper design because the reflection at the two boundaries leads to Fabry-Perot-type oscillations and therefore ripples in the passband of the transmission spectra, resulting in signal distortion. To minimize the reflection, the boundary coupling coefficients should be properly chosen [8]. The coupling coefficients near the boundary can also be apodized to adiabatically transform between the CROW mode and the waveguide modes [9,10].

A further optimization of CROW delay lines consists of a judicious choice of all the coupling coefficients. Each resonator in a CROW can be considered as a feed-back loop which contributes a pole to the transfer function of the CROW. Therefore, the transfer function of an N-resonator CROW is an N-pole optical filter. The coupling coefficients of CROWs can be chosen to achieve desired properties such as maximally flat transmission (Butterworth filters) or maximally flat group delay (Bessel filters) over a prescribed bandwidth. Optical bandpass filters are important elements in optical signal processing, especially for wavelength-division-multiplexed (WDM) systems [11]. High-order bandpass filters based on coupled ring resonators have been extensively studied and experimentally demonstrated [12–16]. Filters based on coupled-resonator systems can also be realized on grating resonators [4,17] and photonic crystal defect resonators [5,18].

A prerequisite for the synthesis of high-order optical filters is a robust and systematic approach to directly relate the desired filter transfer function to the parameters of the CROWs. Several methods have been proposed. For ring or Fabry-Perot resonators, the transfer matrix method (TMM) can be applied to analyze the forward and backward fields inside the

#151208 - $15.00 USD Received 18 Jul 2011; revised 9 Aug 2011; accepted 10 Aug 2011; published 23 Aug 2011

resonators. If the cavity lengths are nearly identical, each delay is an integer multiple of a unit delay, and the CROW can be considered as a digital optical filter and analyzed by the Z-transform formalism [11]. and [19] derived extraction procedures to convert digital filter responses to the field coupling coefficients between ring resonators. A simpler method for the analysis of CROWs is the time-domain coupled-mode theory (CMT), which considers the whole field as a superposition of individual resonator modes and is independent of the type of resonators. The derived coupling coefficients are more general but have to be converted to the parameters of the type of resonators used. In [20], coupling coefficients were extracted by direct comparison of the transfer function derived from CMT and the desired filter response. The approach becomes impractical for high-order filters. Another filter design approach is based on equivalent circuits and the techniques of microwave filters. Circuit-based methods for the synthesis of high-order filters have been proposed in [21] and [22].

In this paper, we present a filter design formalism based on CMT and the recursive properties of the coupling matrix. Coupling coefficients are extracted using recursive relations. In contrast to [20], this formalism does not need a direct comparison and is robust for high-order filters. These universal coupling coefficients can then be converted to the parameters of the specific type of resonators comprising the CROWs. We propose a method for the conversion of the coupling coefficients. This method utilizes the resonance splitting of two coupled resonators for inter-resonator coupling and the transmission of 2-resonator CROWs for waveguide-resonator coupling. It is more accurate than the approaches proposed in [20]. Another interesting property of this formalism is that the time-domain coupling coefficients are proportional to the bandwidth of the filters. For the same kind of filters, the bandwidth can be changed easily without having to rederive the coupling coefficients. We will first describe the formalism for lossless resonators. In the presence of uniform loss or gain, a predistortion technique is applied. We demonstrate the designs of Butterworth and Bessel CROW filters on ring resonators and grating defect resonators.

2. Finite-length CROWs

We start with the theory of CROWs using coupled-mode theory. Figure 1(a) illustrates a CROW with an infinite number of identical resonators. The resonant frequency of each resonator is ω_0, and the inter-resonator coupling coefficient is κ. For an input frequency ω, the mode amplitude of the k-th resonator can be written as $a_k(t)\exp[i\omega t]$, where $a_k(t)$ is the slowly-varying amplitude. $|a_k(t)|^2$ represents the energy stored in the resonator. Since the resonators are coupled only to their neighbors, the coupled-mode equation of each resonator, assumed lossless in this section, can be written as [20,23]

$$\frac{da_k}{dt} = -i\Delta\omega a_k - i\kappa a_{k-1} - i\kappa a_{k+1}, \forall k, \tag{1}$$

where $\Delta\omega \equiv \omega - \omega_0$ and κ is a real number. At steady state, $da_k / dt = 0$, and Eq. (1) becomes a recursive formula for a_k, $\kappa a_{k+1} + \Delta\omega a_k + \kappa a_{k-1} = 0$. The general solution of this recursive formula is $a_{k+1} = \gamma a_k$, where γ is the solution of $\kappa\gamma^2 + (\Delta\omega)\gamma + \kappa = 0$. For a propagating mode (CROW mode), $\gamma = \exp[-iK\Lambda]$, where K is a wave number and Λ is the distance between adjacent resonators. When $|\Delta\omega| < 2\kappa$,

$$\gamma = -\frac{\Delta\omega}{2\kappa} \pm i\sqrt{1-(\frac{\Delta\omega}{2\kappa})^2} = e^{-iK\Lambda}, \tag{2}$$

#151208 - $15.00 USD Received 18 Jul 2011; revised 9 Aug 2011; accepted 10 Aug 2011; published 23 Aug 2011

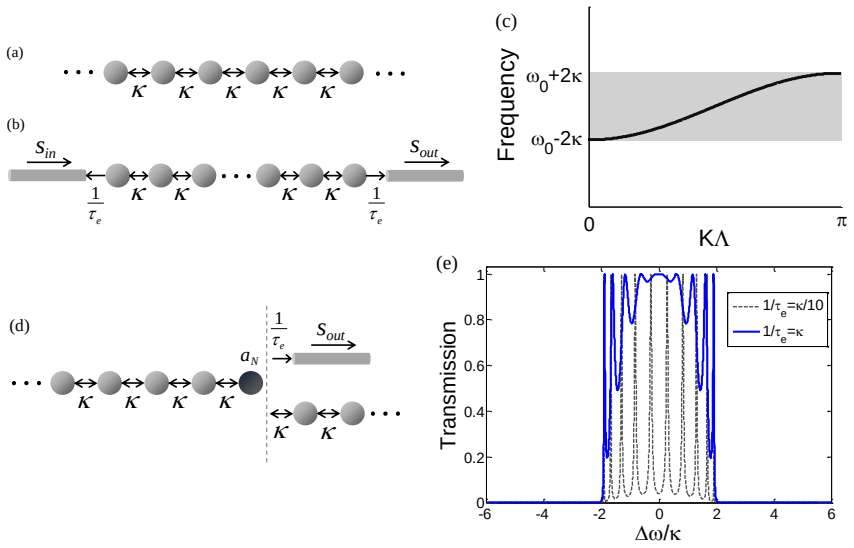

Fig. 1. (a) Schematic drawing of an infinite-length CROW. (b) The dispersion curve of an infinite-length CROW. (c) Schematic drawing of a finite-length CROW. (d) Comparison of a finite-length and an infinite-length CROW at the boundary. (e) Transmission spectra of 10-resonator CROWs with $1/\tau_e = \kappa$ and $1/\tau_e = 0.1\kappa$ respectively.

where $K\Lambda = \pm\cos^{-1}(-\Delta\omega/2\kappa)$. The relation between $\Delta\omega$ and K represents the dispersion curve of the CROW (shown in Fig. 1(b)), which defines the CROW band within which light can propagate. Frequencies outside the CROW band are forbidden since K is complex and $|\gamma| \neq 1$.

In practice, an infinite-length CROW has to be terminated and coupled to the outside world. Shown in Fig. 1(c), the first and last resonators of a CROW are coupled to the input and output waveguides. The coupling to the waveguides can be modeled as external losses, $1/\tau_e$, of the end resonators. When a CROW mode propagates to the boundary, the discontinuity between the CROW and the waveguide causes reflection, leading to Fabry-Perot-type oscillations. The reflection can be minimized by choosing $1/\tau_e$ properly. Figure 1(d) illustrates the difference between a finite-length and an infinite-length CROW at the boundary. In the case of a finite CROW, the N-th resonator is coupled to the output waveguide, while in the case of an infinite CROW, it is coupled to the next resonator. The differential equations for these two cases are respectively

$$\frac{da_N}{dt} = -i\Delta\omega a_N - i\kappa a_{N-1} - \frac{1}{\tau_e} a_N \tag{3a}$$

and

$$\frac{da_N}{dt} = -i\Delta\omega a_N - i\kappa a_{N-1} - i\kappa a_{N+1}. \tag{3b}$$

To match the boundary, the right-hand sides of Eqs. (3)a) and (3b) should be equal so that the N-th resonator cannot tell the termination of the CROW. Since $a_{N+1} = \gamma a_N$ for a CROW mode, the equality of Eqs. (3)a) and (3b) requires

$$\frac{1}{\tau_e} = i\kappa\gamma. \tag{4}$$

#151208 - $15.00 USD Received 18 Jul 2011; revised 9 Aug 2011; accepted 10 Aug 2011; published 23 Aug 2011

For CROW modes, $|\gamma| = 1$. Equation (4) requires $1/\tau_e = \kappa$ and $\gamma = -i$, which corresponds to the center of the CROW band ($\Delta\omega = 0$). Figure 1(e) compares the transmission spectra of 10-resonator CROWs with $1/\tau_e = \kappa$ and $1/\tau_e = 0.1\kappa$ respectively. For $1/\tau_e = \kappa$, the spectrum is flat at the band center. The ripple amplitudes increase at frequencies close to the band edge since the boundary is only matched for $\Delta\omega = 0$. For $1/\tau_e = 0.1\kappa$, the ripples are large over the whole bandwidth. The optimal boundary condition $1/\tau_e = \kappa$ leads to maximally-flat transmission spectrum for finite-size CROWs with uniform coupling coefficients. To further reduce the Fabry-Perot oscillations over the whole CROW band, one can taper the coupling coefficients to adiabatically transform between the CROW mode and the waveguide modes [9,10]. The spectra of transmission and group delay can be further improved by choosing all the coupling coefficients so that the transfer function of the CROW is equal to the transfer function of a desired filter, which will be described in the next section.

3. Synthesis of bandpass filters based on CROWs

Consider a CROW which consists of N identical resonators and is coupled to input and output waveguides (Fig. 2). All the $N + 1$ coupling coefficients are allowed to take on different values. The coupled-mode equations obeyed by the complex amplitudes of the N resonators are

$$\begin{aligned}
\frac{da_1}{dt} &= (-i\Delta\omega - \frac{1}{\tau_{e1}})a_1 - i\kappa_1 a_2 - i\mu_1 s_{in}, \\
\frac{da_2}{dt} &= -i\Delta\omega a_2 - i\kappa_1 a_1 - i\kappa_2 a_3, \\
&\vdots \\
\frac{da_{N-1}}{dt} &= -i\Delta\omega a_{N-1} - i\kappa_{N-2} a_{N-2} - i\kappa_{N-1} a_N, \\
\frac{da_N}{dt} &= (-i\Delta\omega - \frac{1}{\tau_{e2}})a_N - i\kappa_{N-1} a_{N-1}.
\end{aligned} \tag{5}$$

The right-hand side of each equation consists of a detuning term ($-i\Delta\omega a_k$ for each k) and two coupling terms to the neighboring resonators, except for the first and last resonators which have only one neighbor. $1/\tau_{e1}$ and $1/\tau_{e2}$ are external losses of the first and last resonators due to coupling into the waveguides. The input mode with power $|s_{in}|^2$ is coupled into the first resonator via a coupling coefficient μ_1. It can be shown from conservation of energy and time reversal symmetry that $\mu_1 = \sqrt{2/\tau_{e1}}$ [20,24]. At steady state, the left-hand sides of Eq. (5) are all 0. By replacing $i\Delta\omega$ with the Laplace variable s, Eq. (5) can be rewritten as

$$\mathrm{A}\boldsymbol{a} \equiv \begin{bmatrix}
s + \frac{1}{\tau_{e1}} & i\kappa_1 & 0 & 0 & \cdots & 0 \\
i\kappa_1 & s & i\kappa_2 & 0 & \cdots & 0 \\
0 & i\kappa_2 & s & \cdot & \cdot & \cdot \\
\cdot & \cdot & \cdot & \cdot & \cdot & \cdot \\
\cdot & \cdot & \cdot & \cdot & s & i\kappa_{N-1} \\
\cdot & \cdot & \cdot & \cdot & i\kappa_{N-1} & s + \frac{1}{\tau_{e2}}
\end{bmatrix}
\begin{bmatrix} a_1 \\ a_2 \\ \cdot \\ \cdot \\ \cdot \\ a_N \end{bmatrix} =
\begin{bmatrix} -i\mu_1 s_{in} \\ 0 \\ \cdot \\ \cdot \\ \cdot \\ 0 \end{bmatrix}. \tag{6}$$

The $N \times N$ coupling matrix A is a tridiagonal matrix. The vector $\boldsymbol{a}$ which contains all the mode amplitudes can be solved by inverting A. The transmitted and reflected amplitude, s_{out} and s_r are given respectively by

#151208 - $15.00 USD Received 18 Jul 2011; revised 9 Aug 2011; accepted 10 Aug 2011; published 23 Aug 2011

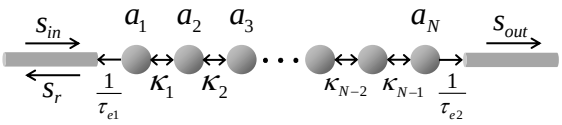

Fig. 2. Schematic drawing of a CROW filter.

$$s_{out} = -i\mu_2 a_N = -\mu_1\mu_2 \left[\mathrm{A}^{-1}\right]_{N,1} s_{in} \tag{7a}$$

and

$$s_r = s_{in} - i\mu_1 a_1 = (1-\mu_1^2 \left[\mathrm{A}^{-1}\right]_{1,1}) s_{in}, \tag{7b}$$

where $\mu_2 = \sqrt{2/\tau_{e2}}$. The amplitude transmission, which is defined as $T \equiv s_{out}/s_{in}$, can be shown as

$$T(s) = -\frac{(-i)^{N-1}\mu_1\mu_2\kappa_1\kappa_2\cdots\kappa_{N-1}}{\det(\mathrm{A})}, \tag{8}$$

where det(A) is the determinant of A and is a polynomial in s with a leading term s^N. Therefore, $T(s)$ is an all-pole function with N poles.

3.1 N-th order all-pole bandpass filters

The transfer function of an all-pole lowpass filter with N poles can be written as

$$T(s) = \frac{k}{s^N + b_{N-1}s^{N-1} + \cdots + b_1 s + b_0}, \tag{9}$$

where $k, b_{N-1}, \ldots, b_0$ are constants. Typical examples of all-pole filters are Butterworth, Chebyshev, and Bessel filters. We substitute s with $i(\omega-\omega_0)/B$, where B is a bandwidth parameter, $T(s)$ then describes a bandpass filter which is centered at ω_0 and of bandwidth scaled by B. Figure 3(a) shows the transmission and group delay spectra of a Butterworth filter and a Bessel filter which feature maximally flat transmission and maximally flat group delay, respectively.

Since the amplitude transmission of an N-resonator CROW (Eq. (8)) and the transfer function of an N-th-order all-pole lowpass filter (Eq. (9)) are both all-pole functions with N poles, we present in what follows a formalism for designing the coupling coefficients of CROWs so that the amplitude transmission of the CROW is equal to the desired $T(s)$.

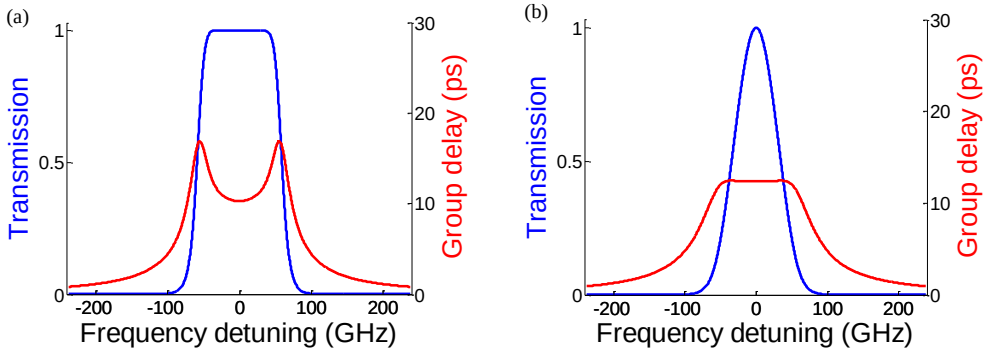

Fig. 3. Spectra of transmission and group delay of (a) a tenth-order Butterworth filter and (b) a tenth-order Bessel filter.

#151208 - $15.00 USD Received 18 Jul 2011; revised 9 Aug 2011; accepted 10 Aug 2011; published 23 Aug 2011

3.2 Extraction of coupling coefficients for a desired filter response

The tridiagonal matrix A in Eq. (6) has the following recursive properties of the polynomials p_1 through p_N:

$$\begin{aligned} p_N &= (s+\frac{1}{\tau_{e1}})p_{N-1} + \kappa_1^{\,2} p_{N-2}, \\ p_{N-1} &= sp_{N-2} + \kappa_2^{\,2} p_{N-3}, \\ &\vdots \\ p_3 &= sp_2 + \kappa_{N-2}^{\,2} p_1, \\ p_2 &= sp_1 + \kappa_{N-1}^{\,2}, \\ p_1 &= s+\frac{1}{\tau_{e2}}, \end{aligned} \quad , \tag{10}$$

where p_k is the determinant of the buttom-right $k \times k$ submatrix of A (a principal minor of A). For example, p_N is the determinant of A, and $p_1 = \mathrm{A}_{N,N}$. Each p_k is a polynomial in s with a leading term s^k. Once we know both p_N and $p_{N\text{-}1}$, all the coupling coefficients $(1/\tau_{e1}, \kappa_1, \kappa_2, \cdots, \kappa_{N-1}, 1/\tau_{e2})$ can be extracted step by step, using Eq. (10). For example, when dividing p_N by $p_{N\text{-}1}$, the quotient is $s+1/\tau_{e1}$, and the remainder is $\kappa_1^{\,2} p_{N-2}$. Then we can continue to divide $p_{N\text{-}1}$ by $p_{N\text{-}2}$.

p_N and $p_{N\text{-}1}$ can be obtained from the transmission and reflection of the CROW. The amplitude transmission $T \equiv s_{out} / s_{in}$ and reflection $R \equiv s_r / s_{in}$ can be shown from Eqs. (7)a) and (7b) as

$$T(s) = \frac{k}{p_N} \tag{11a}$$

and

$$R(s) = \frac{p_N - \mu_1^{\,2} p_{N-1}}{p_N}, \tag{11b}$$

where k is a constant. Given a desired $T(s)$, p_N is already known. To find $p_{N\text{-}1}$, $R(s)$ is also required and can be related to $T(s)$ using conservation of energy, $|T(i\omega)|^2 + |R(i\omega)|^2 = 1$, for a lossless system. Power spectral factorization is performed to obtain $R(s)$ from $|R(i\omega)|^2$. In the power spectral factorization, there are at most 2^N choices of the numerator of $R(s)$, each of which will correspond to different coupling coefficients. We choose the $R(s)$ whose coefficients are real and whose distribution of the zeros is the most symmetric around 0. If $R(s)$ is complex, the resonant frequencies have to be detuned from ω_0, and the resonators are not identical. The details of finding $R(s)$ are described in the appendix.

3.3 Coupling coefficients of Butterworth and Bessel CROWs

Here we use an $N = 4$ Butterworth filter to demonstrate the extraction of coupling coefficients. The transfer function $T(s) = 1/(s^4 + 2.613s^3 + 3.414s^2 + 2.613s + 1)$. The steps are listed in Table 1. For Butterworth filters, the power spectral factorization for solving $R(s)$ is unique and simple. The numerator of $R(s)$ is s^N. Table 2 lists the extracted coupling coefficients for Butterworth and Bessel filters of N = 6 and 10. Note that the extracted coefficients are

#151208 - $15.00 USD Received 18 Jul 2011; revised 9 Aug 2011; accepted 10 Aug 2011; published 23 Aug 2011

normalized by the bandwidth parameter *B*, which can be selected to control the bandwidth of the CROW filter.

The coupling coefficients of Butterworth CROWs are symmetric. At the center of the CROW, the coupling coefficient is about 0.5, which corresponds to a CROW band from $\Delta\omega$ = −1 to 1. The coupling coefficients gradually increase toward the two ends of the CROW. This adiabatic transition of the coupling coefficients reduces the reflection at the boundary, and Butterworth CROWs are one of the optimal designs which remove the oscillations in the transmission spectra. Bessel CROWs, which possess maximally flat delay, do not have symmetric coupling coefficients. With the proper choice of $R(s)$ in the power spectral factorization (see Appendix), the coefficients are nearly symmetric.

Figure 4(a) compares Butterworth CROWs comprising N = 6, 10 and 20. As the order increases, the transmission spectra become flatter in the passband and the roll-off at the band edges is steeper. To see how tolerant the Butterworth CROWs are under random change of the coupling coefficients, Fig. 4(b) shows the transmission spectra of N = 10 Butterworth CROWs whose coupling coefficients are multiplied by a random variable which is uniformly distributed between 0.9 and 1.1. In other words, the standard deviation of the coupling coefficient is 5.8% of its original value. From the transmission spectra of 10 different simulations, the transmission is above 94% over most of the bandwidth.

Table 1. Extraction of Coupling Coefficients for N = 4 Butterworth Filter

$$T(s)=\frac{1}{s^4+2.613s^3+3.414s^2+2.613s+1}=\frac{1}{p_4}\Rightarrow\ |T(i\omega)|^2=\frac{1}{\omega^8+1}\Rightarrow|R(i\omega)|^2=\frac{\omega^8}{\omega^8+1}$$

$$\Rightarrow R(s)=\frac{s^4}{s^4+2.613s^3+3.414s^2+2.613s+1}=\frac{p_4-\mu_1{}^2p_3}{p_4}\Rightarrow p_3=s^3+1.307s^2+s+0.383$$

Divide p_4 by $p_3\Rightarrow p_2=s^2+1.307s+0.707,\ \frac{1}{\tau_{e1}}=1.307,\ \kappa_1=0.841$

Divide p_3 by $p_2\Rightarrow p_1=s+1.307,\ \kappa_2=0.541.$ Divide p_2 by $p_1\Rightarrow\kappa_3=0.841,\ \frac{1}{\tau_{e2}}=1.307$

Table 2. Extracted Coupling Coefficients of Butterworth and Bessel CROW Filters

Filter type	$(1/\tau_{e1},\kappa_1,\kappa_2,\cdots,\kappa_{N-1},1/\tau_{e2})/B$
N = 6 Butterworth	(1.932, 1.169, 0.605, 0.518, 0.605, 1.169, 1.932)
N = 10 Butterworth	(3.196, 1.876, 0.883, 0.630, 0.533, 0.506, 0.533, 0.630, 0.883, 1.876, 3.196)
N = 6 Bessel	(2.068, 1.198, 0.393, 0.397, 0.803, 1.486, 2.427)
N = 10 Bessel	(3.478, 2.030, 0.932, 0.613, 0.305, 0.333, 0.652, 0.772, 1.056, 2.209, 3.745)
N = 10 Butterworth $1/\tau_i=0.05B$	(2.597, 1.575, 0.787, 0.637, 0.412, 0.674, 0.467, 0.588, 0.873, 1.912, 3.296)
N = 10 Butterworth $1/\tau_i=-0.05B$	(3.403, 1.988, 0.921, 0.635, 0.452, 0.474, 0.605, 0.679, 0.955, 2.044, 3.490)

3.4 CROWs with the presence of loss or gain

The filter design formalism described above assumes that the resonators are lossless. In practice, there are loss mechanisms, including intrinsic radiation loss of the resonator design, absorption loss of the material, and scattering loss due to imperfection of the fabrication. The modal loss can be modeled by the loss rate of the resonators, $1/\tau_i$, which is related to the quality factor Q of the resonators by $Q=\omega\tau_i/2$. The differential equation of the k-th resonator in Eq. (5) can be rewritten as

$$\frac{da_k}{dt}=(-i\Delta\omega-\frac{1}{\tau_i})a_k-i\kappa_{k-1}a_{k-1}-i\kappa_k a_{k+1}. \qquad (12)$$

#151208 - $15.00 USD Received 18 Jul 2011; revised 9 Aug 2011; accepted 10 Aug 2011; published 23 Aug 2011

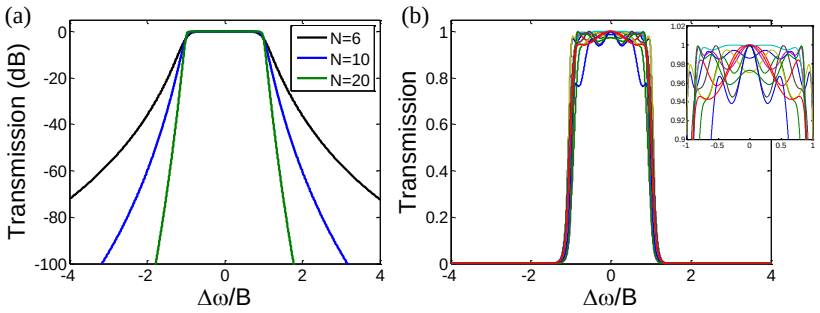

Fig. 4. (a) Transmission spectra of Butterworth CROWs with 6, 10, and 20 resonators. (b) Transmission spectra of N = 10 Butterworth CROWs under random change of coupling coefficients.

If the loss rates of all the resonators are identical, the coupling matrix in Eq. (6) is modified by replacing s with s + $1/\tau_i$. Therefore, for an all-pole filter response $T(s)$ designed for lossless resonators, the transmission in the presence of loss is given by $T'(s) = T(s+1/\tau_i)$, whose poles are shifted to the left by $1/\tau_i$.

To obtain the desired filter response in the presence of loss, the poles can be shifted to the right by $1/\tau_i$ in the design to pre-compensate for the left shift due to the loss. This technique is called predistortion of the filters [25]. First, the poles of the desired function $T(s)$ in Eq. (9) are shifted to the right by $1/\tau_i$. The constant in the numerator has to be decreased so that the magnitude of the new transfer function $T_0(s)$ is always smaller than or equal to 1. As a result, $T_0(s) = \alpha T(s-1/\tau_i)$, where α is a constant and is smaller than 1. In the presence of loss $1/\tau_i$, the transfer function is $T'(s) = T_0(s+1/\tau_i) = \alpha T(s)$, which is recovered to the desired response except for the attenuation factor α.

If the CROW is pumped with uniform gain, the amplifying CROW can be modeled with a negative $1/\tau_i$. The factor α is greater than 1 and is an amplification factor. Table 2 lists the predistorted design for N = 10 Butterworth CROWs with $1/\tau_i$ = 0.05B (lossy) and –0.05B (amplifying) respectively. Their transmission spectra with and without loss/gain are plotted in Figs. 5(a) and 5(b) respectively. Since the group delay is greater at the band edge, frequencies near the band edge experience larger loss and gain. Consequently, the amplitude responses are predistorted accordingly before the loss or gain, as can be seen in Fig. 5. For Bessel filters, since the group delay is almost constant over the bandwidth, the characteristics of the filters remain the same in the presence of small gain or loss.

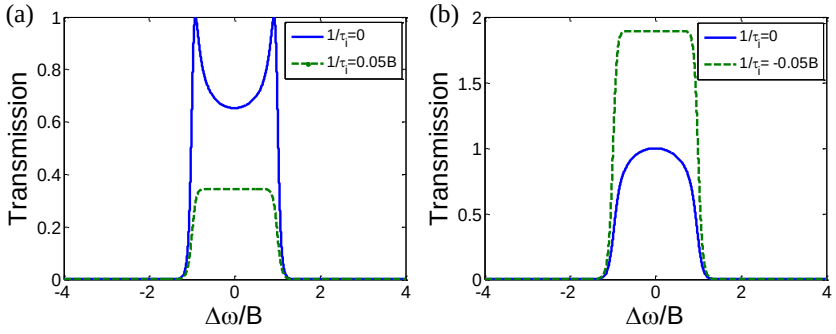

Fig. 5. Transmission spectra of predistorted N = 10 Butterworth CROWs with and without loss/gain for (a) $1/\tau_i = 0.05B$ (loss) and (b) $1/\tau_i = -0.05B$ (gain).

#151208 - $15.00 USD Received 18 Jul 2011; revised 9 Aug 2011; accepted 10 Aug 2011; published 23 Aug 2011

4. CROW filters based on microring resonators

A microring CROW consists of a chain of coupled ring resonators (Fig. 6(a)). Light is coupled in and out of the CROW via the input and output waveguides. Assuming the coupling region is sufficiently long compared to the wavelength, only light circulating in one direction in thering is phase-matched to the input and is excited. The coupling between two adjacent rings can be analyzed, using the notation in Fig. 6(b), by

$$\begin{bmatrix} c_1 \\ c_2 \end{bmatrix} = \begin{bmatrix} t & i\eta \\ i\eta & t \end{bmatrix} \begin{bmatrix} b_1 \\ b_2 \end{bmatrix}, \tag{13}$$

where η and t are respectively the dimensionless coupling and transmission coefficients over the coupling region. Assuming the coupling is lossless, $\eta^2 + t^2 = 1$. The transmission and reflection of microring CROWs can be analyzed using transfer matrix formalism [26].

The field coupling coefficient η at the coupling region is related to the time-domain coupling coefficient κ between two rings. In [20], these relations were derived: $\eta = \kappa / f_{FSR}$ for inter-resonator coupling and $\eta_{in,out} = \sqrt{2/(\tau_e f_{FSR})}$ for waveguide-resonator coupling, where $f_{FSR} = v_g / 2\pi R$ is the free spectral range of the ring resonators. However, these formulas are only valid when the coupling is sufficiently weak, because the field inside the ring is not uniform when η is not much smaller than 1 [15]. In what follows, we describe a method which is valid for any reasonable coupling.

Inter-resonator coupling: Consider two identical resonators coupled to each other with a coupling coefficient κ (Fig. 7(a)). The resonant frequencies of the two eigenmodes are $\omega_0 \pm \kappa$. Figure 7(b) illustrates the corresponding case for ring resonators. The field coupling coefficient is η. The fields $b_{1,2}$ and $c_{1,2}$ are related by the coupling (Eq. (13)), and propagation along the rings leads to

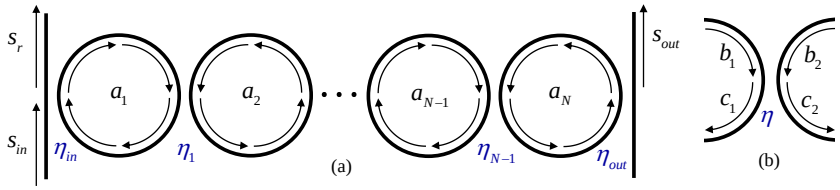

Fig. 6. Schematic drawings of (a) a microring CROW filter and (b) the coupling of two adjacent rings.

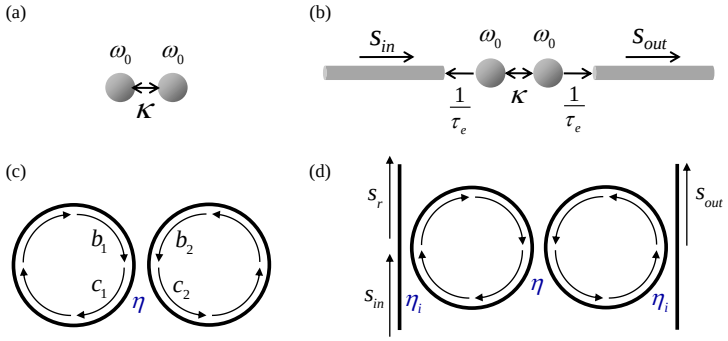

Fig. 7. Schematic drawings of the coupled-resonator structures and the corresponding microring resonators for the derivation of (a,b) inter-resonator coupling and (c,d) waveguide-resonator coupling.

#151208 - $15.00 USD Received 18 Jul 2011; revised 9 Aug 2011; accepted 10 Aug 2011; published 23 Aug 2011

$$\begin{bmatrix} b_1 \\ b_2 \end{bmatrix} = e^{i\theta(\Delta\omega)} \begin{bmatrix} c_1 \\ c_2 \end{bmatrix}, \tag{14}$$

where $\theta(\Delta\omega)$ is the round-trip phase of the rings at $\omega = \omega_0 + \Delta\omega$ and is equal to $-\Delta\omega / f_{FSR}$. Combining Eqs. (13) and (14), $\exp[-i\theta(\Delta\omega)]$ is the eigenvalue of the coupling matrix in Eq. (13), which leads to $\theta(\Delta\omega) = \pm\sin^{-1}\eta$. Therefore, the frequency splitting, which is equal to the coupling coefficient κ, is $\Delta\omega = \pm f_{FSR}\sin^{-1}(\eta)$. As a result,

$$\eta = \sin(\frac{\kappa}{f_{FSR}}). \tag{15}$$

Waveguide-resonator coupling: In Fig. 7(c), the two resonators in Fig. 7(a) are both coupled to an output waveguide with an external loss, $1/\tau_e$. By writing down the coupled-mode equations of the two resonators and solving for the steady-state solution at $\omega = \omega_0$, the amplitude transmission s_{out}/s_{in} is given by $(2\kappa/\tau_e)/(1/\tau_e^2 + \kappa^2)$, which equals 1 only when the boundary condition $1/\tau_e = \kappa$ is satisfied. We can use this structure to derive the conversion of $1/\tau_e$. Figure 7(d) illustrates the corresponding structure for ring resonators. The condition that the transmission is unity at $\omega = \omega_0$ can be derived as

$$\eta_i = \sqrt{\frac{2\eta}{1+\eta}}. \tag{16}$$

For a given $1/\tau_e$, we first use Eq. (15) to find an inter-resonator coupling η which corresponds to a coupling coefficient $\kappa = 1/\tau_e$, and then use Eq. (16) to obtain η_i.

With Eqs. (15) and (16), we are ready to convert the coupling coefficients κ in Table 2 to the microring couplings η. The only constraint is that κ does not exceed $(\pi/2)f_{FSR}$, or $\omega_{FSR}/4$, the maximal coupling which ring resonators with a free spectral range f_{FSR} can achieve (see Eq. (15)). We consider examples of silicon microring CROWs. The mode index and group index of the silicon waveguides are respectively 2.4 and 4. The ring radius is 30 μm so that one resonant wavelength is at 1570.8 nm, and the free spectral range f_{FSR} is 398 GHz. The bandwidth of the filters can be chosen by setting the bandwidth parameter B. For example, the bandwidth of Butterworth filters is $2B$ (Fig. 3(a)). If we choose $B = \omega_{FSR}\cdot 0.005$, where $\omega_{FSR} = 2\pi f_{FSR}$, the bandwidth is $2\cdot 398\text{GHz}\cdot 0.005 = 3.98\text{GHz}$. The converted η for Butterworth and Bessel filters with $B = \omega_{FSR}\cdot 0.005$ and $B = \omega_{FSR}\cdot 0.05$ are listed in Table 3.

The transmission spectra of the microring CROWs in Table 3 were calculated using the transfer matrix formalism and were compared with the original transmission spectra based on the κ in Table 2, calculated using CMT. Figure 8(a) shows the transmission spectra of Butterworth filters with $B = \omega_{FSR}\cdot 0.005$. Since η are sufficiently weak (the largest η is 0.338), the two spectra are nearly identical. Figure 8(b) shows the spectra for $B = \omega_{FSR}\cdot 0.05$, where the coupling is stronger. Although there are small passband ripples whose amplitude is about 0.0002, the spectrum still closely agrees with the desired response. Therefore, the conversion is valid even when η is as high as 0.852, whereas the same κ would be converted to $\eta = 1.102$ using the formula proposed in [20]. Note that for a bigger bandwidth or higher filter order, κ at the boundary will increase and might exceed the upper limit of κ, $(\pi/2)f_{FSR}$. Therefore, resonators with large f_{FSR} are beneficial. However, for ring resonators with very small radii, say less than 5 μm, the assumption of the transfer matrix formalism that the coupling region is sufficiently long compared to the wavelength is no long valid, and the coupling of modes will be complicated since modes in the opposite direction will also be excited. Figure 8(c) shows the spectra of transmission and group delay for an $N = 6$ Bessel CROW with $B = \omega_{FSR}\cdot 0.05$. Figure 8(d) compares the transmission spectra of Butterworth CROWs with 6 and 20 rings.

#151208 - $15.00 USD Received 18 Jul 2011; revised 9 Aug 2011; accepted 10 Aug 2011; published 23 Aug 2011

Table 3. Coupling Coefficients of Microring CROW Filters

Filter type	Bandwidth	$(\eta_{in},\eta_1,\eta_2,\cdots,\eta_5,\eta_{out})$
N = 6 Butterworth	$B=\omega_{FSR}\cdot 0.005$	(0.338, 0.0367, 0.0190, 0.0163, 0.0190, 0.0367, 0.338)
	$B=\omega_{FSR}\cdot 0.05$	(0.852, 0.359, 0.189, 0.162, 0.189, 0.359, 0.852)
N = 6 Bessel	$B=\omega_{FSR}\cdot 0.005$	(0.349, 0.0376, 0.0123, 0.0125, 0.0252, 0.0467, 0.376)
	$B=\omega_{FSR}\cdot 0.05$	(0.868, 0.368, 0.123, 0.124, 0.250, 0.450, 0.904)

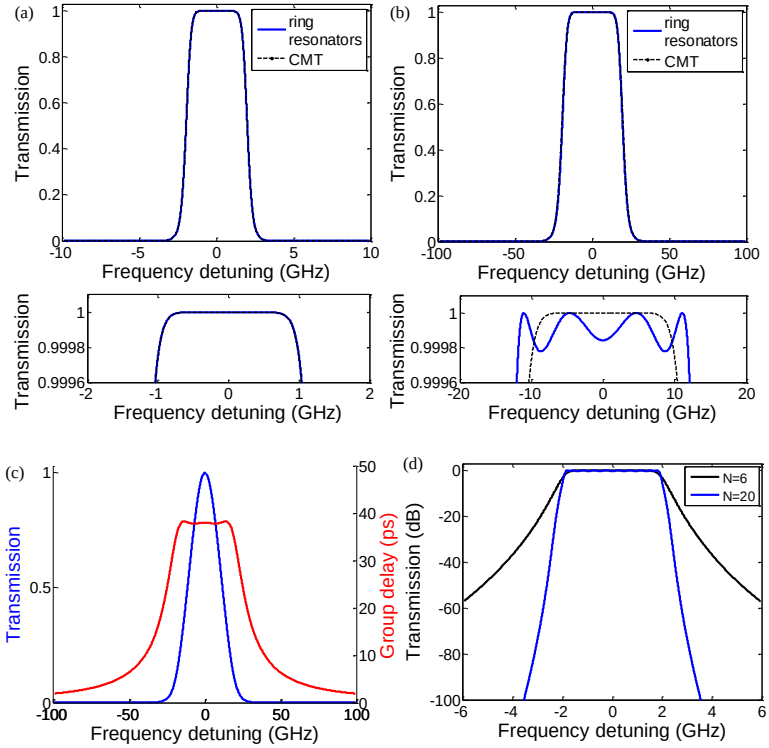

Fig. 8. (a,b) Transmission spectra and their enlarged passband spectra of N = 6 Butterworth microring CROW filters with (a) $B = \omega_{FSR}\cdot 0.005$ and (b) $B = \omega_{FSR}\cdot 0.05$. (c) Transmission and group delay of an N = 6 Bessel microring CROW. (d) Transmission spectra of Butterworth microring CROWs with 6 and 20 resonators respectively.

5. CROW filters based on grating defect resonators

CROWs can be realized on a waveguide grating with multiple "defects". A Bragg grating is a periodic perturbation to the waveguide. When an artificial defect is introduced in a grating, a defect mode is created with a resonant frequency inside the grating band gap. If the defect length corresponds to a quarter wavelength (a quarter-wave-shifted defect), the mode resonates at the Bragg frequency of the grating. This defect mode consists of a forward and a backward waveguide mode. The envelope of the field distribution is centered at the defect and decays exponentially in the grating, as shown in Fig. 9(a). If the grating consists of multiple defects (Fig. 9(b)), each defect mode interacts with its neighbors via their evanescent tails. The coupling between adjacent defects can be controlled by the spacing between the defects (L_1,L_2,…,L_{N+1} in Fig. 9(b)). These defect resonators form a grating CROW.

#151208 - $15.00 USD Received 18 Jul 2011; revised 9 Aug 2011; accepted 10 Aug 2011; published 23 Aug 2011

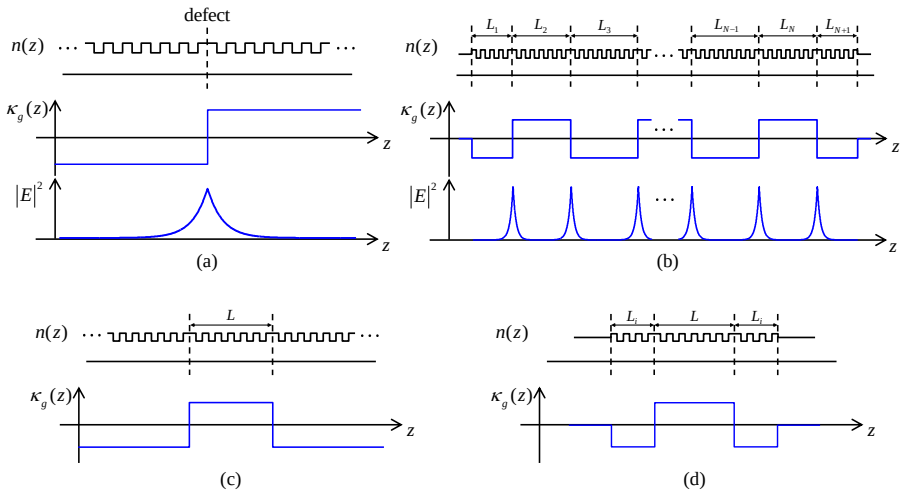

Fig. 9. Distribution of refractive index, coupling coefficient, and the envelope of intensity along z of (a) a defect resonator, (b) a grating CROW, (c) two coupled defect resonators, and (d) two coupled defect resonators with external coupling to the waveguide.

CROWs based on waveguide gratings are attractive because the coupling between CROWs and waveguides is natural and easy to implement. For strong gratings, the size of grating resonators can be as small as several microns, which is much smaller compared to ring resonators [4]. However, the defect resonators in a strong grating require a proper design to reduce the radiation losses due to spatial Fourier components which are coupled to the radiation modes of the waveguide [27].

CROWs based on weak gratings can be analyzed by coupled-mode equations [17,28]:

$$\begin{aligned} \frac{da(z)}{dz} &= -i\delta a(z) + i\kappa_g^{*}(z)b(z), \\ \frac{db(z)}{dz} &= i\delta b(z) - i\kappa_g(z)a(z), \end{aligned} \tag{17}$$

where a and b are the amplitudes of the forward and backward waveguide modes, δ is the detuning of the propagation constant from the Bragg condition of the grating, and $\kappa_g(z)$ is the coupling coefficient of the grating. In a grating CROW, the phase of $\kappa_g(z)$ is shifted by π at each quarter-wave-shifted defect, as shown in Fig. 9(b), while the amplitude remains the same. For an input mode $a(-\infty)$ from the left, the field distribution and the transmission of a grating CROW with a given $\kappa_g(z)$ can be solved using Eq. (17) with the boundary condition $b(\infty) = 0$.

The conversion from the coupling coefficients κ in Table 2 to the lengths $L_1, L_2, \ldots, L_{N+1}$ in grating CROWs applies methods similar to those employed in Section 4.

Inter-resonator coupling: Fig. 9(c) shows the case of two defects which are separated by a distance L in an infinitely long grating. It was shown in [17] that under the assumption of $\exp(-\kappa_g L) \ll 1$, the resonance splitting due to the coupling is $\Delta\omega = \pm\kappa_g v_g \exp(-\kappa_g L)$, where v_g is the group velocity of the waveguide mode. Since the $\Delta\omega$ is equal to the coupling coefficient κ of the two resonators,

$$L = -\frac{1}{\kappa_g}\ln\left(\frac{\kappa}{\omega_g}\right), \tag{18}$$

where $\omega_g \equiv \kappa_g v_g$.

#151208 - $15.00 USD Received 18 Jul 2011; revised 9 Aug 2011; accepted 10 Aug 2011; published 23 Aug 2011

Waveguide-resonator coupling: Fig. 9(d) shows a finite grating with two defects. The external loss $1/\tau_e$ of the defect modes into the waveguides is controlled by the length L_i. The amplitude transmission of this grating at Bragg frequency can be solved, using Eq. (17), as $1/\cosh[\kappa_g(2L_i - L)]$. The transmission is unity if $L_i = L/2$, which corresponds to the boundary condition $\kappa = 1/\tau_e$. Therefore,

$$L_i = -\frac{1}{2\kappa_g}\ln(\frac{1/\tau_e}{\omega_g}). \tag{19}$$

Using Eqs. (18) and (19), the coupling coefficients in Table 2 are converted to the lengths of the grating sections, which are listed in Table 4. We consider Si waveguides whose group index is 4 at the wavelength of 1570 nm. The grating strength κ_g is 0.1/μm, so $\omega_g/(2\pi)$ is 1.19 THz. The transmission and group delay spectra of N = 6 Butterworth and Bessel filters with $B = \omega_{FSR}\cdot 0.05$ are plotted in Fig. 10.

Table 4. Lengths of Grating Sections for Grating CROW Filters

Filter type	Bandwidth	$(L_1, L_2, \cdots, L_{N+1})$
N = 6 Butterworth	$B = \omega_g \cdot 0.05$	(11.7, 28.4, 35.0, 36.5, 35.0, 28.4, 11.7) μm
	$B = \omega_g \cdot 0.005$	(23.2, 51.4, 58.0, 59.6, 58.0, 51.4, 23.2) μm
N = 6 Bessel	$B = \omega_g \cdot 0.05$	(11.3, 28.1, 39.3, 39.2, 32.1, 26.0, 10.5) μm
	$B = \omega_g \cdot 0.005$	(22.9, 51.2, 62.3, 62.2, 55.2, 49.0, 22.1) μm

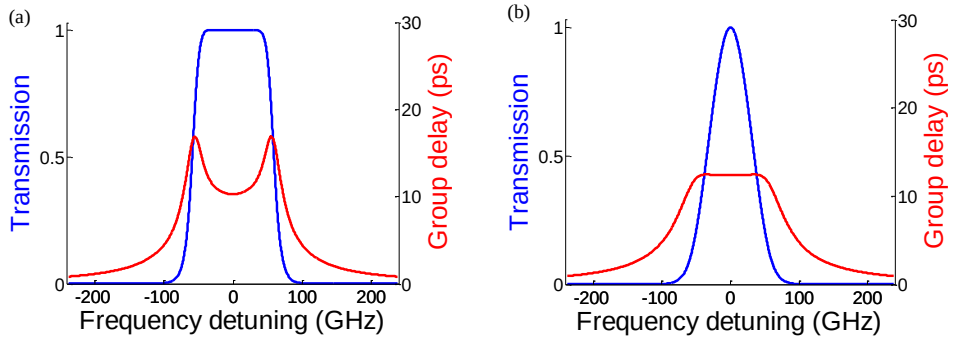

Fig. 10. Transmission and group delay spectra of (a) an N = 6 Butterworth grating CROW filter and (b) an N = 6 Bessel grating CROW filter.

6. Conclusion

We have demonstrated a formalism for choosing the coupling coefficients of CROWs to achieve desired filter responses such as maximally flat transmission (Butterworth filters) and maximally flat group delay (Bessel filters). The formalism uses CMT and the recursive relations of the coupling matrix to extract the coupling coefficients. Compared to TMM, the design using CMT is simpler since the field in each resonator is represented by only one variable. The universal coupling coefficients can be applied to any type of resonators or even the coupling of different types of resonators. The bandwidth of the filters can be changed easily by selecting the bandwidth parameter B. Furthermore, predistortion techniques can be applied for the design of lossy or amplifying CROW filters.

The disadvantage of CMT is that it assumes weak coupling between resonators and that the field distribution in each resonator remains unchanged. It is less accurate than TMM, which directly analyzes the fields inside the resonators. The time-domain coupling coefficients of CMT have to be converted to the parameters of the type of resonators comprising the CROWs. We have demonstrated the conversion to the field coupling

#151208 - $15.00 USD Received 18 Jul 2011; revised 9 Aug 2011; accepted 10 Aug 2011; published 23 Aug 2011

coefficients for microring resonators and the lengths of grating sections for grating defect resonators. The formulas for the conversion are valid for any reasonable coupling.

Appendix

In what follows we describe the details of finding p_{N-1} for the purpose of using Eq. (10) to extract the coupling coefficients of CROWs. The formalism is similar to the z-domain digital filter design described in [11,19].

Assuming the CROW is lossless, $T(s)$ and $R(s)$ are related by ... For an all-pole filter of order N, $T(s)$ can be written as

$$T(s) = \frac{k}{(s-q_1)(s-q_2)\cdots(s-q_N)}, \tag{20}$$

where q_1 through q_N are the poles and k is a constant. All the filter responses $T(s)$ we consider in this paper are real functions, so the poles come in complex conjugate pairs. Therefore,

$$\left|T(i\omega)\right|^2 = \frac{k^2}{(\omega^2+q_1{}^2)(\omega^2+q_2{}^2)\cdots(\omega^2+q_N{}^2)}, \tag{21}$$

and

$$\left|R(i\omega)\right|^2 = 1-\left|T(i\omega)\right|^2 = \frac{(\omega^2+q_1{}^2)(\omega^2+q_2{}^2)\cdots(\omega^2+q_N{}^2)-k^2}{(\omega^2+q_1{}^2)(\omega^2+q_2{}^2)\cdots(\omega^2+q_N{}^2)}. \tag{22}$$

The denominators of $T(s)$ and $R(s)$ are identical, as can be seen in Eqs. (11)a) and (11b). We assume that the numerator of $R(s)$ is $p(s) = (s-z_1)(s-z_2)\cdots(s-z_N)$, where z_1 through z_N are the zeros of $R(s)$. The goal of power spectral factorization is to find z_1 through z_N so that $\left|p(i\omega)\right|^2 = (\omega^2+q_1{}^2)(\omega^2+q_2{}^2)\cdots(\omega^2+q_N{}^2)-k^2$. Each zero z_i is selected from a pair (z, $-z^*$), where z is a complex number, so there are at most 2^N combinations of zeros. In general, $p(s)$, and thus p_{N-1}, are not real. For a filter with a complex p_{N-1}, the resonant frequencies of the resonators have to be detuned, and Eq. (6) is modified as

$$\mathrm{A}\boldsymbol{a} \equiv \begin{bmatrix} s-i\delta_1+\frac{1}{\tau_{e1}} & i\kappa_1 & 0 & 0 & \cdots & 0 \\ i\kappa_1 & s-i\delta_2 & i\kappa_2 & 0 & \cdots & 0 \\ 0 & i\kappa_2 & s-i\delta_3 & \cdot & \cdot & \cdot \\ \cdot & \cdot & \cdot & \cdot & \cdot & \cdot \\ \cdot & \cdot & \cdot & \cdot & s-i\delta_{N-1} & i\kappa_{N-1} \\ \cdot & \cdot & \cdot & \cdot & i\kappa_{N-1} & s-i\delta_N+\frac{1}{\tau_{e2}} \end{bmatrix} \begin{bmatrix} a_1 \\ a_2 \\ \cdot \\ \cdot \\ \cdot \\ a_N \end{bmatrix} = \begin{bmatrix} -i\mu_1 s_{in} \\ 0 \\ \cdot \\ \cdot \\ \cdot \\ 0 \end{bmatrix}, \tag{23}$$

where $\delta_i \equiv \omega_i - \omega_0$ is the frequency detuning of each resonator from ω_0. Equation (10) is also modified by replacing s with $s-\delta_i$, so δ_i can be extracted during the extracting process.

The zeros of $R(s)$ can be chosen so that p_{N-1} is real. Figure 11 shows three different choices of zeros for an $N = 7$ Bessel filter. They correspond to different coupling coefficients κ and frequency detuning δ, as listed in Table 5. The first one is often referred to as "minimum phase", where all zeros are located inside the left-half s-plane (Fig. 11(a)). It corresponds to zero frequency detuning and monotonically increasing κ. In the second one, the zeros are all located at the first and third quadrants (Fig. 11(b)). The resulting values of κ are symmetric, but the frequency detuning is nonzero since p_{N-1} is complex. In our CROW filter design, we

#151208 - $15.00 USD Received 18 Jul 2011; revised 9 Aug 2011; accepted 10 Aug 2011; published 23 Aug 2011

prefer a nearly symmetric κ without frequency detuning. Consequently, we choose the zeros that are the most uniformly distributed around the origin and are complex conjugate pairs, as shown in Fig. 11(c). Note that although the three CROW filters in Table 5 look very different, they have the same $T(s)$ and $\left|R(i\omega)\right|^2$, except that the phase of $R(s)$ is different.

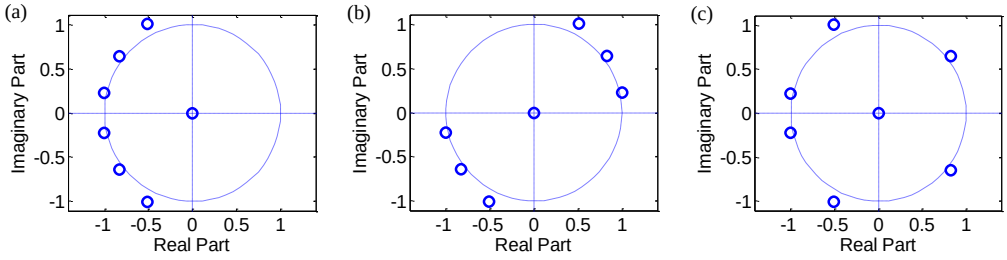

Fig. 11. Choices of zeros for R(s). (a) Minimum phase. (b) 1st and 3rd quadrants. (c) Nearly uniform distribution.

Table 5. Coupling Coefficients and Frequency Detuning of N = 7 Bessel CROW Filters with Different Choices of Zeros

Choice of zeros	$\bar{\kappa} = (1/\tau_{e1}, \kappa_1, \kappa_2, \cdots, \kappa_{N-1}, 1/\tau_{e2})/B,\ \bar{\delta} = (\delta_1, \delta_2, \cdots, \delta_N)/B$
Minimum phase	$\bar{\kappa}$ = (0.241, 0.345, 0.557, 0.699, 0.899, 1.320, 2.876, 4.937) $\bar{\delta}$ = (0, 0, 0, 0, 0, 0, 0)
1st and 3rd quadrants	$\bar{\kappa}$ = (2.589, 1.460, 0.619, 0.486, 0.486, 0.619, 1.460, 2.589) $\bar{\delta}$ = (0.495, 0.514, 0.461, 0.000, –0.461, –0.514, –0.495)
Nearly uniform distribution	$\bar{\kappa}$ = (1.898, 1.174, 0.390, 0.357, 0.684, 0.932, 1.926, 3.280) $\bar{\delta}$ = (0, 0, 0, 0, 0, 0, 0)

Acknowledgments

This work was supported by National Science Foundation and The Army Research Office.

#151208 - $15.00 USD Received 18 Jul 2011; revised 9 Aug 2011; accepted 10 Aug 2011; published 23 Aug 2011